Supporting Information A (SI-A) to:

Chlorothalonil Transformation Products in Drinking Water Resources: Widespread and Challenging to Abate

Karin Kiefer[1,2], Tobias Bader[3], Nora Minas[1], Elisabeth Salhi[1], Elisabeth M.-L. Janssen[1], Urs von Gunten[1,2,4], Juliane Hollender[1,2]*

[1]Eawag, Swiss Federal Institute of Aquatic Science and Technology, 8600 Dübendorf, Switzerland
[2]Institute of Biogeochemistry and Pollutant Dynamics, ETH Zurich, 8092 Zurich, Switzerland
[3]Laboratory for Operation Control and Research, Zweckverband Landeswasserversorgung, 89129 Langenau, Germany
[4]School of Architecture, Civil and Environmental Engineering (ENAC), École Polytechnique Fédérale de Lausanne (EPFL), 1015 Lausanne, Switzerland

*Corresponding author: juliane.hollender@eawag.ch

Water Research, 2020

Table of Contents

SI-A1: Selected Waterworks

Table SI-A1: Investigated waterworks and details on treatment steps.

Waterworks	Raw Water	Treatment Steps
A	River Rhine	1) Rapid sand filter 2) Granular activated carbon filtration (GAC) in parallel o GAC 1: specific throughput 25 m^3kg^{-1} GAC o GAC 2: specific throughput 55 m^3kg^{-1} GAC o GAC 3: specific throughput 305 m^3kg^{-1} GAC 3) UV disinfection (medium pressure lamp, Berson Inline, > 400 Jm^{-2})
B	Groundwater (karstic spring)	1) Ozonation (0.8 g O_3 g^{-1} DOC) 2) Multi-layer filtration (no sampling) 3) GAC filtration in parallel o GAC 1: specific throughput 23 m^3kg^{-1} GAC o GAC 2: specific throughput 216 m^3kg^{-1} GAC o 2 more GAC filters (no sampling) 4) ClO_2 disinfection (no sampling)
C	Lake water	1) Pre-Ozonation (0.3 g O_3 g^{-1} DOC) 2) Rapid sand filtration (no sampling) 3) Intermediate ozonation (0.6 g O_3 g^{-1} DOC) 4) GAC filtration: specific throughput 1200 m^3kg^{-1} GAC 5) Slow sand filtration
D	River water	1) River bank filtration 2) Cl_2/ClO_2 disinfection (0.3-0.4 mgL^{-1}) 3) Artificial recharge and abstraction
E	Groundwater	• 2 abstraction wells influenced by river bank filtration o Distance to river: 40 m o UV disinfection (medium pressure lamp, Barrier® M, > 400 Jm^{-2}) • 1 abstraction well (no further treatment) o Distance to river: 730 m • 1 abstraction well o Not influenced by river o Reverse osmosis pilot plant
F	Groundwater	• 1 abstraction well (no further treatment) • 2 springs (no further treatment) • 1 spring o UV disinfection (low pressure lamp, Aquafides 1 AF300 T, > 400 Jm^{-2})
G	Groundwater	• 1 Groundwater abstraction well (no further treatment) • 1 Groundwater spring (no further treatment)
I	Groundwater	• Groundwater abstraction well (no further treatment) • Water is mixed (ratio 1:1, v:v) with groundwater from area with low agricultural impact

SI-A2: Stock Solutions

Analyte stock solutions for LC-MS/MS analysis: Reference material was dissolved depending on solubility and stability (Table SI-A2). Then, mixed solutions were prepared in ethanol at different concentrations.

Table SI-A2: Analyte stock solutions in organic solvent.

Analyte	Solvent	Concentration
Chlorothalonil TP R471811-SA	Ethanol:Water (1:1, v:v)	1000 mgL^{-1}
Chlorothalonil TP R417888-SA	Methanol	1000 mgL^{-1}
Chlorothalonil TP R419492-SA	Ethanol:Water (1:1, v:v)	100 mgL^{-1}
Chlorothalonil TP SYN507900-Ph	Ethanol:Water (1:1, v:v)	100 mgL^{-1}
Chlorothalonil TP R611968-Ph	Ethanol	1000 mgL^{-1}
Chlorothalonil TP SYN5458580-Ph	Ethanol:Water (1:1, v:v)	100 mgL^{-1}
Acesulfame	Ethanol:Water (1:1, v:v)	1000 mgL^{-1}
Diatrizoic acid	Ethanol	1000 mgL^{-1}
Salicylic acid	Acetonitrile	1000 mgL^{-1}

Isotope-labelled internal standards: Isotope-labelled internal standards were dissolved in ethanol, methanol, acetonitrile, ethanol/water mix, methanol/water mix, dimethyl sulfoxide, ethyl acetate, toluene, acetone, water at concentrations ranging from 100 to 1000 mgL^{-1}, depending on the solubility and stability. Then, mixed solutions were prepared in ethanol or acetonitrile at 10 mgL^{-1}, which were combined for the final spike solution (0.1 mgL^{-1}).

Aqueous stock solutions for laboratory experiments: Aqueous stock solutions (20-100 µM) were prepared using the stock solutions described in Table SI-A2. The organic solvent was evaporated under a gentle nitrogen stream. Then, the precipitate was dissolved in ultrapure water at room temperature within one to two days. The aqueous stock solution was stored until the experiment (up to seven days) at 4 °C.

SI-A3: LC-MS/MS and LC-UV Settings

Environmental samples were enriched using vacuum-assisted evaporative concentration, whereas samples from laboratory experiments were analysed without enrichment. Table SI-A3 and Table SI-A4 describe the HPLC-HRMS/MS method used for the environmental samples and samples from experiments with UV irradiation, ozone and hydroxyl radicals ($^{\cdot}OH$). The adsorption experiment with activated carbon was performed at the Laboratory for Operation Control and Research (Zweckverband Landeswasserversorgung) and samples were subsequently measured onsite with a different HPLC-MS/MS method (Table SI-A5, Table SI-A6, and Table SI-A7). The actinometer atrazine used for the photodegradation experiments was analysed by HPLC-UV (Table SI-A8).

Table SI-A3: HPLC method for environmental samples and samples from experiments with UV irradiation, ozone and ·OH.

Autosampler: PAL RTC (CTC Analytics, Switzerland) **Pump: Dionex UltiMate3000 RS (Thermo Fisher Scientific, U.S.)** **Column: Atlantis T3 3 µm, 3.0 x 150 mm (Waters, Ireland)**	
Injection volume	150 µL (environmental samples) 100 µL (laboratory samples)
Flow rate	0.3 mL min^{-1}
Eluent A	Water + 0.1% concentrated formic acid
Eluent B	Methanol + 0.1% concentrated formic acid
Gradient	0 min: 100% eluent A, 0% eluent B 1.5 min: 100% eluent A, 0% eluent B 18.5 min: 5% eluent A, 95% eluent B 28.5 min: 5% eluent A, 95% eluent B 29 min: 100% eluent A, 0% eluent B 33 min: 100% eluent A, 0% eluent B

Table SI-A4: ESI-HRMS/MS settings for environmental samples and samples from experiments with UV irradiation, ozone and ·OH.

Mass spectrometer: Fusion Lumos (Thermo Fisher Scientific, U.S.)	
Spray voltage (kV)	3.5 / -2.5
Capillary temperature (°C)	300
Sheath gas (AU)	40
Auxiliary gas (AU)	10
S-lens RF level (AU)	60
Automatic gain control (AGC) target MS1	5×10^4
Maximum injection time MS1 (ms)	50
Scan range MS1 (m/z)	100 - 1000
Resolution MS1 (at m/z 200)	240 000
Internal calibration	Yes (Easy-IC)
Cycle time	1 s
MS/MS activation type	Higher energy collisional dissociation (HCD)
Data-dependent trigger	Ions of target compounds; if idle pick most intense
Isolation window (m/z)	1
Resolution MS2 (at m/z 200)	30 000
Automatic gain control (AGC) target MS2	1×10^4
Maximum injection time MS2 (ms)	54
Dynamic exclusion time (s)	3
Normalized collision energy (NCE)	Stepped: 20, 40, 60 or 20, 30, 40

Table SI-A5: HPLC method for samples from laboratory experiments with activated carbon.

Autosampler: Nexera X2 SIL-30AC (Shimadzu, Japan) **Pump: Nexera X2 LC-30AD** **Column: Ultra Aqueous C18 5 µm, 4.6x250 mm (Restek, U.S.)**	
Injection volume	100 µL
Flow rate	0.8 $mLmin^{-1}$
Eluent A	Water + 0.1% concentrated formic acid
Eluent B	Acetonitrile + 0.1% concentrated formic acid
Gradient	0 min: 98% eluent A, 2% eluent B 7 min: 20% eluent A, 80% eluent B 12 min: 20% eluent A, 80% eluent B 12.1 min: 98% eluent A, 2% eluent B 17 min: 98% eluent A, 2% eluent B

Table SI-A6: Parameter settings for triple quadrupole measurement for samples from laboratory experiments with activated carbon.

Mass spectrometer: API 5500 Qtrap (Sciex, U.S.)	
Ion Spray Voltage	4500 / -4500
Curtain Gas	30
Collision Gas	Medium
Temperature	700
Ion Source Gas 1	50
Ion Source Gas 2	60
Entrance Potential	10 / -10

Table SI-A7: Parameter settings for triple quadrupole measurement for samples from laboratory experiments with activated carbon.

Analyte	**Q1 → Q3** **In Da**	**Dwell time** **in ms**	**DP** **in V**	**CE** **in V**	**CXP** **in V**
Chlorothalonil TP	345 → 302	50	-100	-40	-12
R471811-SA	345 → 238	50	-100	-40	-12
Chlorothalonil TP	327 → 220	50	-60	-36	-9
R417888-SA	327 → 284	50	-60	-26	-13
Chlorothalonil TP	263 → 35	50	-135	-70	-17
SYN507900-Ph	263 → 184	50	-135	-40	-11
	283 → 220	50	-135	-28	-11
Chlorothalonil TP	263 → 35	50	-45	-78	-17
R611968-Ph	263 → 156	50	-45	-46	-7
	263 → 184	50	-45	-34	-11
Diatrizoic acid	615 → 361	30	101	47	18
	615 → 233	30	101	55	12
Atrazine	216 → 174	30	46	27	8
	216 → 104	30	46	27	8

Table SI-A8: HPLC-UV method for actinometry with atrazine.

Autosampler: Dionex UltiMate3000 RS (Thermo Fisher Scientific, U.S.) **Pump: Dionex UltiMate3000 RS (Thermo Fisher Scientific, U.S.)** **Column: Atlantis T3 3 µm, 3.0 x 150 mm (Waters, Ireland)** **Detector: Diode Array, Dionex UltiMate3000 RS (Thermo Fisher Scientific, U.S.)**	
Injection volume	100 µL
Flow rate	0.3 $mLmin^{-1}$
Eluent A	Water + 0.1% concentrated formic acid
Eluent B	Acetonitrile + 0.1% concentrated formic acid
Gradient	0 min: 50% eluent A, 50% eluent B 7 min: 5% eluent A, 95% eluent B 9 min: 5% eluent A, 95% eluent B 9.5 min: 50% eluent A, 50% eluent B 13.5 min: 50% eluent A, 50% eluent B
Wavelength	265 nm

SI-A4: Quantification

SI-B1 and SI-B2 summarizes quantification results and various analytical information such as limit of quantification (LOQ), isotope-labelled internal standards (ILIS), or relative recoveries for the environmental samples. For other samples (laboratory experiments, pilot plant reverse osmosis), LOQ, ILIS and relative recovery may differ (e.g. due to different analytical methods).

ILIS Selection: Quantification was based on the peak area ratio of analyte and ILIS. If a structurally identical ILIS was not available (i.e. for all chlorothalonil TPs), ILIS selection was supported by an internal R script using the R functions available on Zenodo (Schollée 2018). First, the TraceFinder 4.1 export was imported to R (R Core Team 2016) and all ILIS co-eluting with the analyte within the given RT window (±2.5 min) were selected (function selectISTDs()). Then, a linear calibration model was calculated for each combination of analyte and ILIS (function calibrationCalc()), and finally, sample concentrations were determined based on each calibration model (function predictConc()). Using the concentration c in the spiked / not spiked samples and the theoretical spike level, relative recoveries as defined in equation (SI-1) were calculated,

$$\text{Relative Recovery} = \frac{\left(c_{\text{spiked sample}} - c_{\text{not spiked sample}}\right)}{\text{Theoretical Spike Level}} \quad \text{(SI-1)}$$

if the following equation was true (function recoveryCalc()):

$$c_{\text{not spiked sample}} < \left(c_{\text{spiked sample}} - c_{\text{not spiked sample}}\right) \cdot 1.7 \quad \text{(SI-2)}$$

This check ensured that relative recoveries were only determined if the concentration difference in the spiked and not spiked samples was large enough, to avoid cases where the relative recoveries were dominated by measurement uncertainty, and therefore, misleading. Finally, an ILIS was selected for which the mean relative recovery was close to 100% and the standard deviation of the relative recoveries across the spiked samples was low. Final analyte concentrations were corrected by the relative recovery, if a structurally identical ILIS was not available.

Limit of Quantification (LOQ): The LOQ in ultrapure water ($LOQ_{Ultrapure}$) was defined as the lowest calibration standard with at least five data points along the chromatographic peak (MS1 full scan mode) and a peak area ratio (analyte vs. ILIS) of at least twice the peak area ratio in all blank samples. To estimate the LOQ in matrix (LOQ_{Matrix}), the $LOQ_{Ultrapure}$ was divided by the absolute recovery:

$$LOQ_{Matrix} = \frac{LOQ_{Ultrapure}}{\text{Absolute Recovery}} \quad \text{(SI-3)}$$

If the sample concentration was in the range of the LOQ_{Matrix}, the so-defined LOQ_{Matrix} was lowered if the chromatographic peaks in the samples were defined by at least five data points.

Absolute recoveries were determined for each analyte by comparing the peak area in the matrix to the peak area in ultrapure water, as described in the following. If a structurally identical ILIS was available (i.e. for acesulfame), the peak area of the ILIS in the matrix (environmental samples) was divided by the peak area of the ILIS in ultrapure water (median of all enriched calibration standards) according to equation 4:

$$\text{Absolute Recovery}_{\substack{\text{Identical}\\\text{ILIS}}} = \text{Median}\,\frac{\text{Peak Area ILIS}_{\text{Matrix}}}{\text{Median (Peak Area ILIS}_{\text{Ultrapure}})} \quad \text{(SI-4)}$$

If a structurally identical ILIS was not available (i.e. all chlorothalonil TPs), the peak area of the analyte in the spiked sample (after subtracting the peak area in the not spiked sample) was compared to the peak area of the analyte in the calibration standard that corresponded to the spike level:

$$\text{Absolute Recovery}_{\substack{\text{No Identical}\\\text{ILIS}}} = \frac{\text{Peak Area}_{\substack{\text{Spiked}\\\text{Sample}}} - \text{Peak Area}_{\substack{\text{Not Spiked}\\\text{Sample}}}}{\text{Peak Area}_{\substack{\text{Calibration}\\\text{Standard}}}} \quad \text{(SI-5)}$$

SI-A5: UVC Irradiation

Figure SI-A1 illustrates the absorbance spectra of the chlorothalonil TPs and the emission spectrum of the UVC lamps. UVC irradiation experiments were conducted in triplicate at pH 7.5 (actinometer atrazine: pH 7.0). The experiments with the phenolic TPs were repeated with shorter irradiation time to capture more data points for the assessment of the phototransformation rate for these fast degrading compounds. The determined photon fluence rates at the two different days differed by 25% (4.0×10^{-5} and 5.3×10^{-5} E m^{-2} s^{-1}), which can be the result of small variations of performance of the lamps, temperature in the reactor, distance of the vials to the lamps, etc.

The reported phototransformation data (Table SI-A9) was determined as follows. First, the pseudo-first-order phototransformation rate constants k_{obs} (s^{-1}) for each TP and for the actinometer atrazine were determined from a linear regression (Figure SI-A2) according to equation (SI-6):

$$\ln\left(\frac{[TP]_T}{[TP]_0}\right) = -\,k_{obs}t \quad \text{(SI-6)}$$

Then, the photon fluence rate E was calculated from k_{obs} of the actinometer atrazine according to:

$$E = \frac{k_{obs}^{atr}}{2.303\;\Phi_{atr}\;\varepsilon_{atr\;254nm}}\ \text{(einstein}\ m^{-2}s^{-1}\text{)}, \quad \text{(SI-7)}$$

where Φ_{atr} and $\varepsilon_{atr\ 254nm}$ are the quantum yield (0.046 mol E^{-1}, Hessler et al. (1993)) and molar absorptivity at wavelength 254 nm (3860 M^{-1} cm^{-1} Nick et al. (1992) of atrazine.

The quantum yield Φ_{TP} of each TP was obtained according to equation (SI-8)

$$\Phi_{TP} = \Phi_{atr}\,\frac{k_{obs}^{TP}}{k_{obs}^{atr}}\,\frac{\varepsilon_{254\ nm}^{atr}}{\varepsilon_{254\ nm}^{TP}}\ \text{(mol einstein}^{-1}\text{)} \quad \text{(SI-8)}$$

In addition, the photon fluence based rate constants k_E^{TP} were calculated:

$$k_E^{TP} = \frac{k_{obs}^{TP}}{E}\ \text{(m}^2\ \text{einstein}^{-1}\text{)} \quad \text{(SI-9)}$$

Photon fluence based rate constants are independent of the experimental set-up and allow therefore a comparison with other studies (Canonica et al. 2008).

Furthermore, we calculated the relative abatement in UV disinfection and UV/H_2O_2 assuming only direct photolysis and a UV dose of 400 Jm^{-2} (=8.49 10^{-4} einstein m^{-2}) and 7500 Jm^{-2} (=1.59 10^{-2} einstein m^{-2}), respectively (Canonica et al. 2008):

$$\text{relative abatement (254 nm, 400 Jm}^{-2}\text{)} = 1 - \exp\left(-k_E^{TP}\ 8.49\ 10^{-4}\ \text{einstein m}^{-2}\right) \quad \text{(SI-10)}$$

$$\text{relative abatement (254 nm, 7500 Jm}^{-2}\text{)} = 1 - \exp\left(-k_E^{TP}\ 1.59\ 10^{-2}\ \text{einstein m}^{-2}\right) \quad \text{(SI-11)}$$

Additionally, we determined the UV dose necessary to remove 90% of the TPs (Table SI-A10) as described by Bahnmüller et al. (2015):

$$\text{UV dose (90\% abatement)} = \frac{-\ln(0.1)}{k_E^{TP}}\ 4.75 \times 10^5\ \text{J einstein}^{-1}\ \ (\text{J m}^{-2}) \quad \text{(SI-12)}$$

The factor 4.75×10^5 is the photon to energy conversion factor for 254 nm.

Table SI-A9: Determined photochemical data: observed pseudo-first-order phototransformation rate constants of the actinometer atrazine or the chlorothalonil TP (k_{obs}^{atr}, k_{obs}^{TP}), photon fluence rate E, molar absorptivity $\varepsilon_{254\,nm}^{TP}$, and the quantum yield Φ_{TP}. Standard deviation of quantum yields consider the propagated standard deviation of the measured rates of the actinometer and of the TPs, potential standard error of the absorbance spectra were not considered.

	R471811-SA	**R417888-SA**	**R611968-Ph**	**SYN507900-Ph**
k_{obs}^{atr} in s^{-1}	$(2.2\pm0.1) \times 10^{-3}$	$(2.2\pm0.1) \times 10^{-3}$	$(1.6\pm0.1) \times 10^{-3}$	$(1.6\pm0.1) \times 10^{-3}$
E in einstein $m^{-2}s^{-1}$	$(5.3\pm0.1) \times 10^{-5}$	$(5.3\pm0.1) \times 10^{-5}$	$(4.0\pm0.1) \times 10^{-5}$	$(4.0\pm0.1) \times 10^{-5}$
k_{obs}^{TP} in s^{-1}	$(6.0\pm0.3) \times 10^{-5}$	$(9.9\pm0.2) \times 10^{-5}$	$(6.9\pm0.1) \times 10^{-4}$	$(11.6\pm0.1) \times 10^{-4}$
k_E^{TP} in m^2einstein^{-1}	1.1±0.1	1.9±0.1	17±1	29±1
$\varepsilon_{254\,nm}^{TP}$ in $M^{-1}cm^{-1}$	710	8000	5400	6900
Φ_{TP} in mol einstein^{-1}	$(0.7\pm0.1) \times 10^{-2}$	$(0.10\pm0.01) \times 10^{-2}$	$(1.4\pm0.1) \times 10^{-2}$	$(1.8\pm0.1) \times 10^{-2}$
Rel. Abatement in % at 254 nm, 400 Jm^{-2}	0.1	0.2	1.5	2.4

Table SI-A10: Relative abatement for different fluence doses applied for UV disinfection (400 Jm^{-2}) and UV-based AOPs (7500 Jm^{-2}), as well as calculated fluence doses required to remove 90% of chlorothalonil TPs by UVC treatment in water without organic matter and nitrate.

	Relative abatement for 400 Jm^{-2} in %	Relative abatement for 7500 Jm^{-2} in %	UV dose for 90% abatement in Jm^{-2}
R471811-SA	0.1	1.8	968000
R417888-SA	0.2	2.9	588000
SYN507900-Ph	2.4	37	38000
R611968-Ph	1.5	24	64000

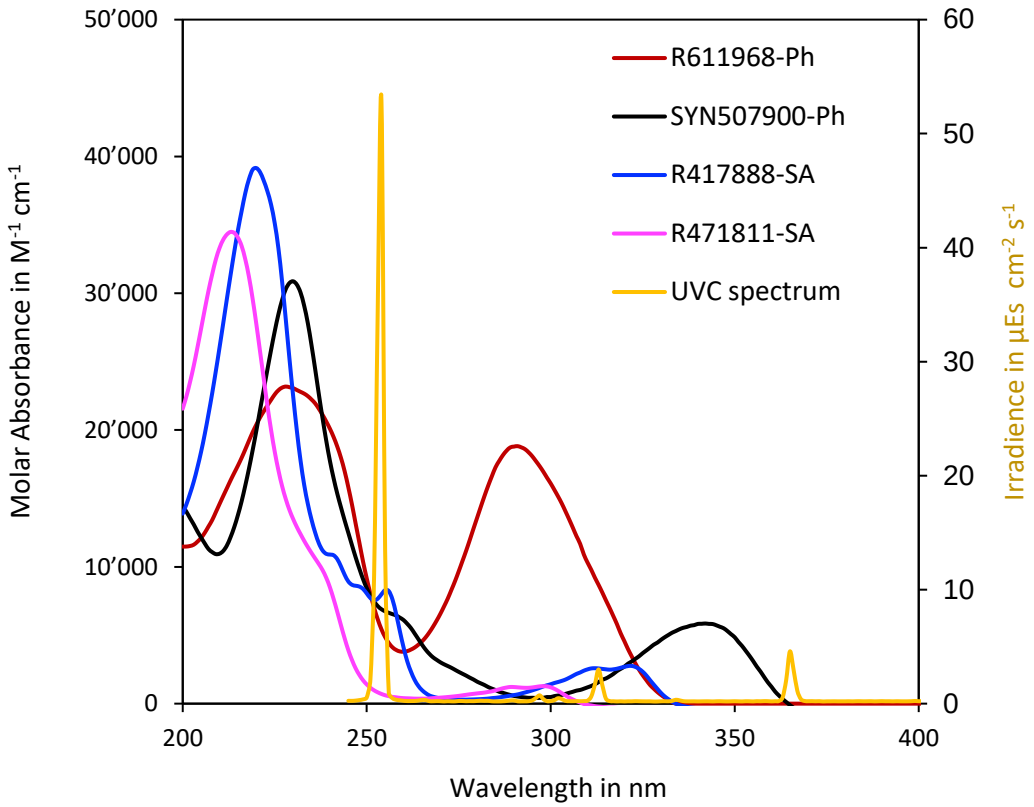

Figure SI-A1: Absorbance spectra of the chlorothalonil TPs (R611968-Ph: 20 µM, SYN507900-Ph: 20 µM, R417888-SA: 50 µM, R471811-SA: 50 µM, path length: 1 cm) and emission spectrum of the UVC lamps with peak emission at 254 nm.

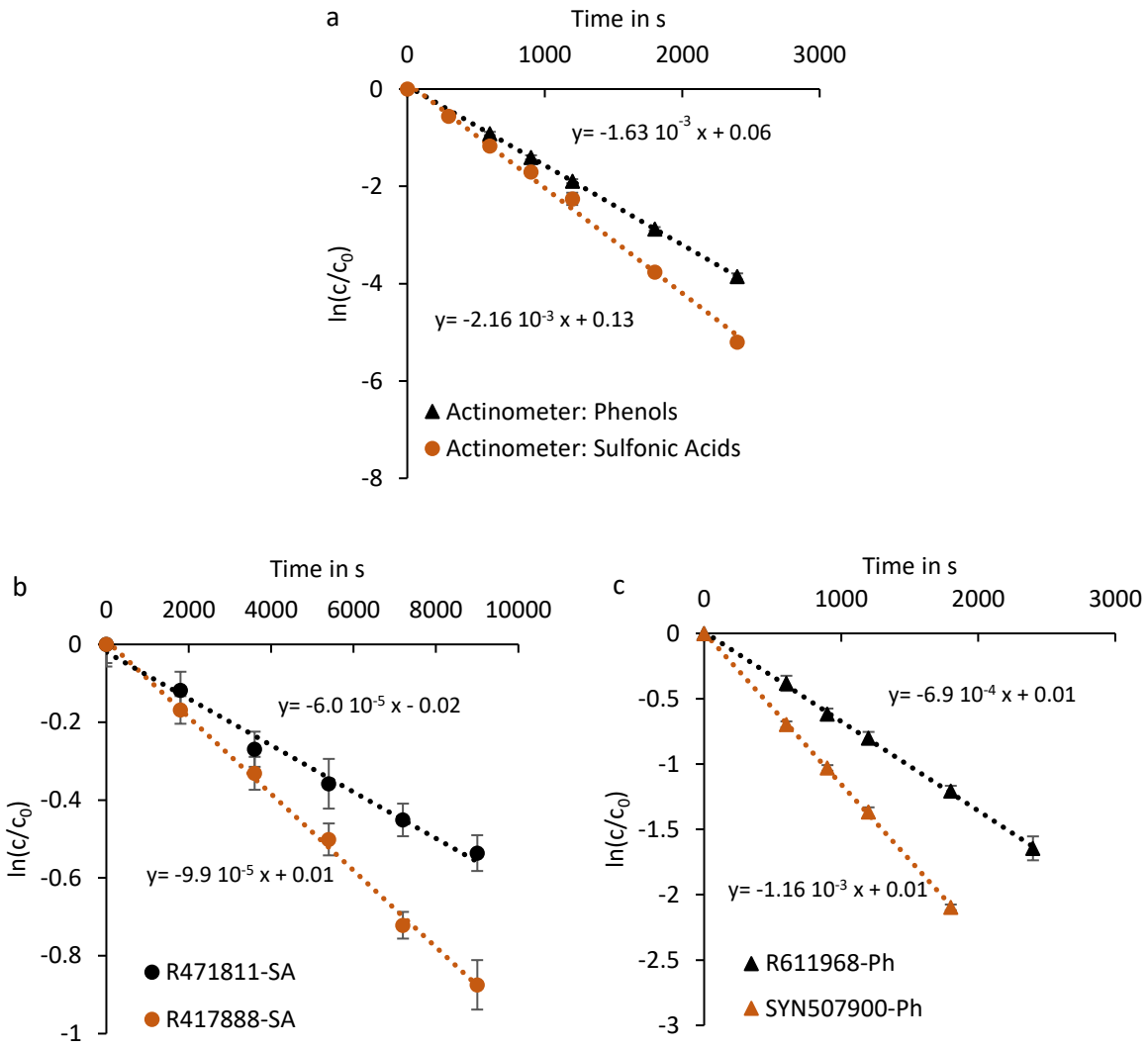

Figure SI-A2: Phototransformation observed in UVC experiments (a) of the actinometer atrazine in experiments with phenolic TPs and sulfonic acid TPs, (b) of the sulfonic acids R471811-SA and R417888-SA, and (c) of the phenolic TPs R611968-Ph and S YN507900-Ph. Error bars indicate standard deviations of triplicates. Temperature: 12±2 °C. pH: 7.5 for chlorothalonil TPs and 7.0 for actinometer atrazine (phosphate buffer). Chlorothalonil TPs: 0.1 µM. Atrazine: 5 µM.

SI-A6: Ozone Experiments with Sulfonic Acids

Ozone stock solutions were prepared by sparging an ozone/oxygen gas mixture produced by an ozone generator from pure oxygen (BMT 803 BT, BMT Messtechnik GmbH, Germany) into ice-cooled ultra-purified water (Bader and Hoigné 1981). The ozone concentration was determined either with the indigo method (Bader and Hoigné 1981) or spectrophotometrically using the absorbance at 260 nm (ε = 3200 $M^{-1}cm^{-1}$) (von Sonntag and von Gunten 2012). To determine the second order rate constant (k_{O3}) for the reaction of ozone with the slowly-reacting sulfonic acid TPs (R471811-SA, R417888-SA), the TPs were exposed to ozone in excess at pH 2.3 (0.1 µM TP, 100 µM ozone, 10 mM phosphoric acid) in a 250 mL glass bottle with a dispenser system (Hoigné and Bader 1994). Acidic conditions were selected as ozone is more stable at low pH (von Sonntag and von Gunten 2012) and the sulfonic acid

TPs do not change their speciation over a wide pH range (predicted pK_a -4.3). To scavenge $^{\cdot}OH$, *tert*-butanol (10 mM) was added to the solution. To monitor TP abatement and the ozone concentration, eleven samples were collected at various time points over 15 h. Directly after sampling, ozone was quenched using 3-buten-2-ol (210 µM, to determine the TP concentration) or indigo trisulfonate (100 µM, to determine the ozone concentration).

The ozone concentration decreased exponentially, whereas the TPs were stable (Figure SI-A3). The second order rate constant k_{O3}^{TP} was estimated from the ozone exposure ($\int[O_3]\,dt$) according to equation (SI-13) (von Gunten and Hoigne 1994) and assuming that TP degradation was $\leq 10\%$:

$$\ln\left(\frac{[TP]_t}{[TP]_0}\right) = -k_{O3}^{TP} \int [O_3]\,dt \qquad \text{(SI-13)}$$

$$\Leftrightarrow \quad k_{O3}^{TP} < -\frac{\ln(0.9)}{\int_0^{53520} 111\, e^{-4\,10^{-5}t}\,dt} \approx -\frac{\ln(0.9)}{2.4\,10^6\ \mu M\ s} \approx 0.04\ M^{-1}s^{-1} \qquad \text{(SI-14)}$$

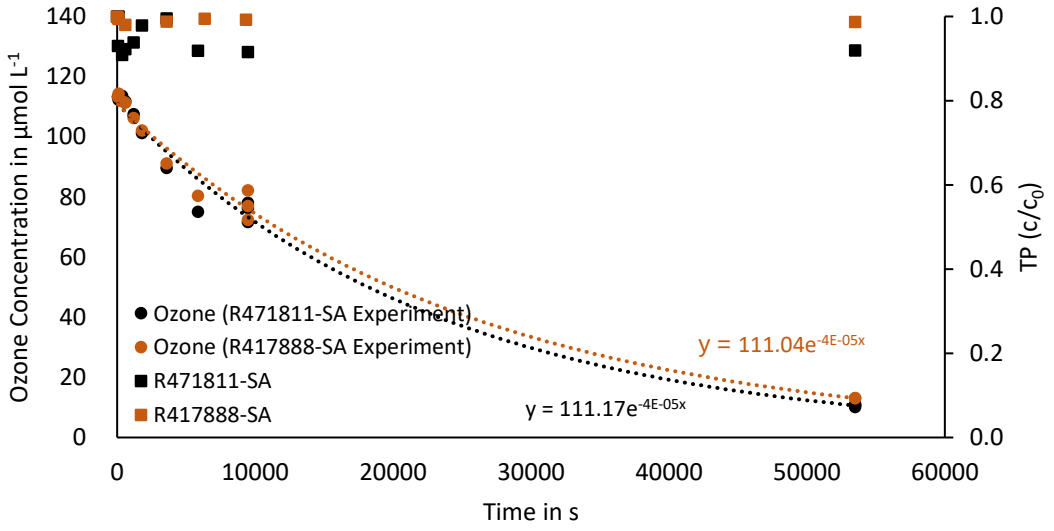

Figure SI-A3: Decrease of ozone (circles) in ozonation batch experiment with the sulfonic acids R471811-SA and R417888-SA. The concentration of R471811-SA and R417888-SA was constant within measurement uncertainty. Temperature: 23 ± 2 °C. pH: 2.3. Concentration of TPs: 0.1 µM.

SI-A7: Ozone Experiments with Phenols

Determination of second order rate constants: The kinetics of the reactions of the faster reacting phenolic TPs (SYN507900-Ph, R611968-Ph) were investigated by competition kinetics using salicylic acid as competitor. The phenolic TPs (1 µM) and salicylic acid (1 µM) were exposed in three independent experiments to varying ozone doses (0-2 µM, 0-4.5 µM and 0-6 µM) at pH 7.5 in 10 mL glass vials. To scavenge $^{\cdot}OH$, 50 mM *tert*-butanol was added before the experiment. The rate constant was derived from linear regression according to equation (SI-15):

$$\ln\left(\frac{[TP]_x}{[TP]_0}\right) = \frac{k_{O3}^{TP}}{k_{O3}^{competitor}} \ln\left(\frac{[competitor]_x}{[competitor]_0}\right) \quad \text{(SI-15)}$$

where $[TP]_x$, $[TP]_0$, $[competitor]_x$ and $[competitor]_0$ are the concentration of the chlorothalonil TP or competitor at varying ozone doses or without ozone, respectively, and k are the second order rate constants for the reaction of ozone with the TP or the competitor. The second order rate constant for salicylic acid was obtained from Hoigné and Bader (1983). It should be noted that Hoigné and Bader (1983) reported conflicting values (Table 1: (2.8±3) × 10^3 $M^{-1}s^{-1}$, Table 2: (3.0±1.0) × 10^4 $M^{-1}s^{-1}$; Figure 4: ~3 × 10^3 $M^{-1}s^{-1}$). For the calculations in this study, we used k_{O3} = 2.8 × 10^4 $M^{-1}s^{-1}$, because it is reported both in a Table and a Figure. However, the uncertainty in the second order rate constant may affect the determined second order rate for the reaction of ozone with the phenolic TPs by a factor of 10.

The reported rate constant and uncertainty is the average and standard deviation of the rate constants calculated from the three experiments (Table SI-A11). In case of SYN507900-Ph, one rate constant was considered as outlier (factor 2.8 lower) and therefore was not used to calculate the final second order rate constant. This discrepancy can be explained by the fact that the experimental conditions were not optimized at that point (ozone doses too low, 0-2 µM).

Table SI-A11: Second order rate constants calculated from experiments conducted with varying ozone doses (0-2 µM, 0-4.5 µM and 0-6 µM); *outlier.

TP	Rate Constant 1 in $M^{-1}s^{-1}$	Rate Constant 2 in $M^{-1}s^{-1}$	Rate Constant 3 in $M^{-1}s^{-1}$	**Average Rate Constant in $M^{-1}s^{-1}$**
R611968-Ph	2.43 × 10^4	3.01 × 10^4	2.40 × 10^4	(2.6 ± 0.3) × 10^4
SYN507900-Ph	1.50 10^4 *	4.22 10^4	4.05 10^4	4.1 10^4

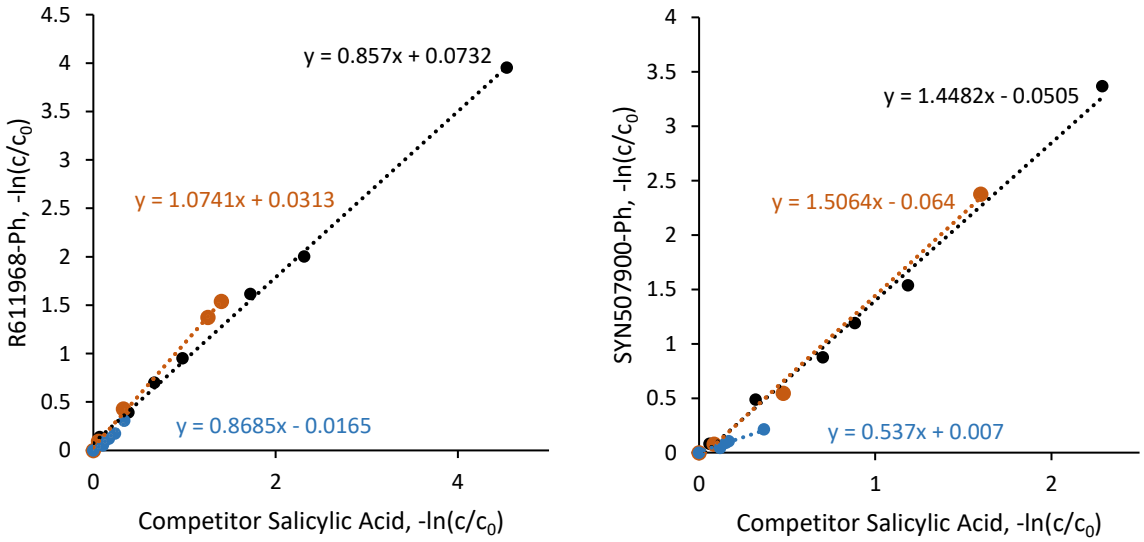

Figure SI-A4: Competition kinetics plots for the phenolic TPs and the competitor salicylic acid in presence of ozone; orange: 0-6 µM ozone; black: 0-4.5 µM ozone; blue: 0-2 µM ozone. Temperature: 23 ± 2 °C. pH: 7.5 (5 mM phosphate buffer). Concentrations of TPs and competitor: 1 µM.

Estimation of second order rate constants with QSAR: Lee and von Gunten (2012) developed quantitative structure-activity relationships (QSARs) to predict second order rate constants for the reactions of ozone with e.g. phenols based on substituent descriptors (Hammett constants σ, σ^+, σ^-). For phenols (PhOH) and phenolates (PhO^-), Lee and von Gunten (2012) proposed the QSAR equations (SI-16) and (SI-17):

$$\log k_{O3}^{PhOH} = 3.53\ (\pm 0.25) - 3.24(\pm 0.69) \sum \sigma^+_{o,m,p} \qquad \text{(SI-16)}$$

$$\log k_{O3}^{PhO^-} = 8.80\ (\pm 0.16) - 2.27(\pm 0.30) \sum \sigma^+_{o,m,p} \qquad \text{(SI-17)}$$

Using the Hammett constants collected by Lee and von Gunten (2012) and references therein for the substituents of the phenolic chlorothalonil TPs (Table SI-A12), second order rate constants were predicted (Table SI-A13). The predicted rate constants for the dissociated phenolic TPs, which are the major form (> 99%) at pH 7.5 due to the low predicted pK_a values (4.1-4.7; JChem for Office, Version 17.1.2300.1455, ChemAxon Ltd.) were higher by a factor of 2.3-2.5 compared to the measured values. This is in the range of the uncertainties described by Lee and von Gunten (2012). The phenolic TP SYN548580-Ph was not investigated in laboratory experiments. The second-order rate constant predicted by QSAR was $2.9 \times 10^5\ M^{-1}s^{-1}$.

Table SI-A12: Hammett constants for ortho, meta and para position. *σ^+ values were not available and therefore replaced by σ values. σ^+ (vs. σ) accounts for resonance effects (Lee and von Gunten 2012).

Substituents	**σ^+_o**	**σ^+_m**	**σ^+_p**
-Cl	0.07	0.40	0.11
-CN	0.44	0.56	0.66
-CONH2	0.24*	0.28*	0.36*

Table SI-A13: Substituents of the phenolic TPs, measured k_{O3} (pH 7.5) and predicted k_{O3} for the phenol (PhOH) and the dissociated phenol (PhO^-).

TP	**ortho**	**meta**	**para**	$\sum \sigma^+_{o,m,p}$	**k_{O3} pH 7.5**	**k_{O3}^{PhOH}**	**k_{O3}^{PhO-}**
R611968-Ph	Cl, CONH2	Cl, Cl	CN	1.77	2.61×10^4	6.23×10^{-3}	6.10×10^4
SYN507900-Ph	Cl, CN	Cl, Cl	CONH2	1.67	4.14×10^4	1.33×10^{-2}	1.04×10^5
SYN548580-Ph	Cl, CONH2	Cl, Cl	CONH2	1.47		5.84×10^{-2}	2.92×10^5

SI-A8: Advanced Oxidation Experiments with Sulfonic Acids

To generate sufficiently high $^{\cdot}OH$ concentrations, the relatively stable sulfonic acid TPs were exposed to ozone (0-80 µM) at pH ~10 (0.3 mM NaOH). It should be noted that R417888-SA was not completely stable at pH ~10, i.e. a slight formation of R471811-SA (2%) was observed (for each ozone dose, including the control without ozone addition). However, this did not affect the interpretation of the experiments because each sample (with corresponding ozone dose) was affected to the same extent.

Diatrizoic acid (k_{OH} 5.4 x 10^8 $M^{-1}s^{-1}$, Real et al. (2009)) was used as competitor. In addition, one experiment was performed in which the two TPs R471811-SA and R417888-SA were exposed to ozone (0-210 µM) together (R471811-SA as competitor instead of diatrizoic acid, Figure SI-A5). The second order rate constants were calculated according to equation (SI-18) and are summarized in Table SI-A14:

$$\ln\left(\frac{[TP]_x}{[TP]_0}\right) = \frac{k_{OH}^{TP}}{k_{OH}^{competitor}} \ln\left(\frac{[competitor]_x}{[competitor]_0}\right) \quad \text{(SI-18)}$$

The competitor diatrizoic acid reacts approximately ten times faster than the sulfonic acids, leading to higher uncertainties, but experiments conducted with both TPs together confirmed the results.

Table SI-A14: Second order rate constants *k* calculated from experiments conducted with varying ozone doses.

TP	Competitor	$k_{competitor}$ in $M^{-1}s^{-1}$	$k_{target\ compound}$ in $M^{-1}s^{-1}$	**Reported $k_{target\ compound}$ in $M^{-1}s^{-1}$**
R471811-SA	Diatrizoic acid	5.4×10^8	$\sim 3.0 \times 10^7$	$< 5.0 \times 10^7$
R417888-SA	Diatrizoic acid	5.4×10^8	$\sim 1.7 \times 10^7$	$< 5.0 \times 10^7$
R417888-SA	R471811-SA	$\sim 3.0 \times 10^7$	$\sim 1.7 \times 10^7$	$< 5.0 \times 10^7$

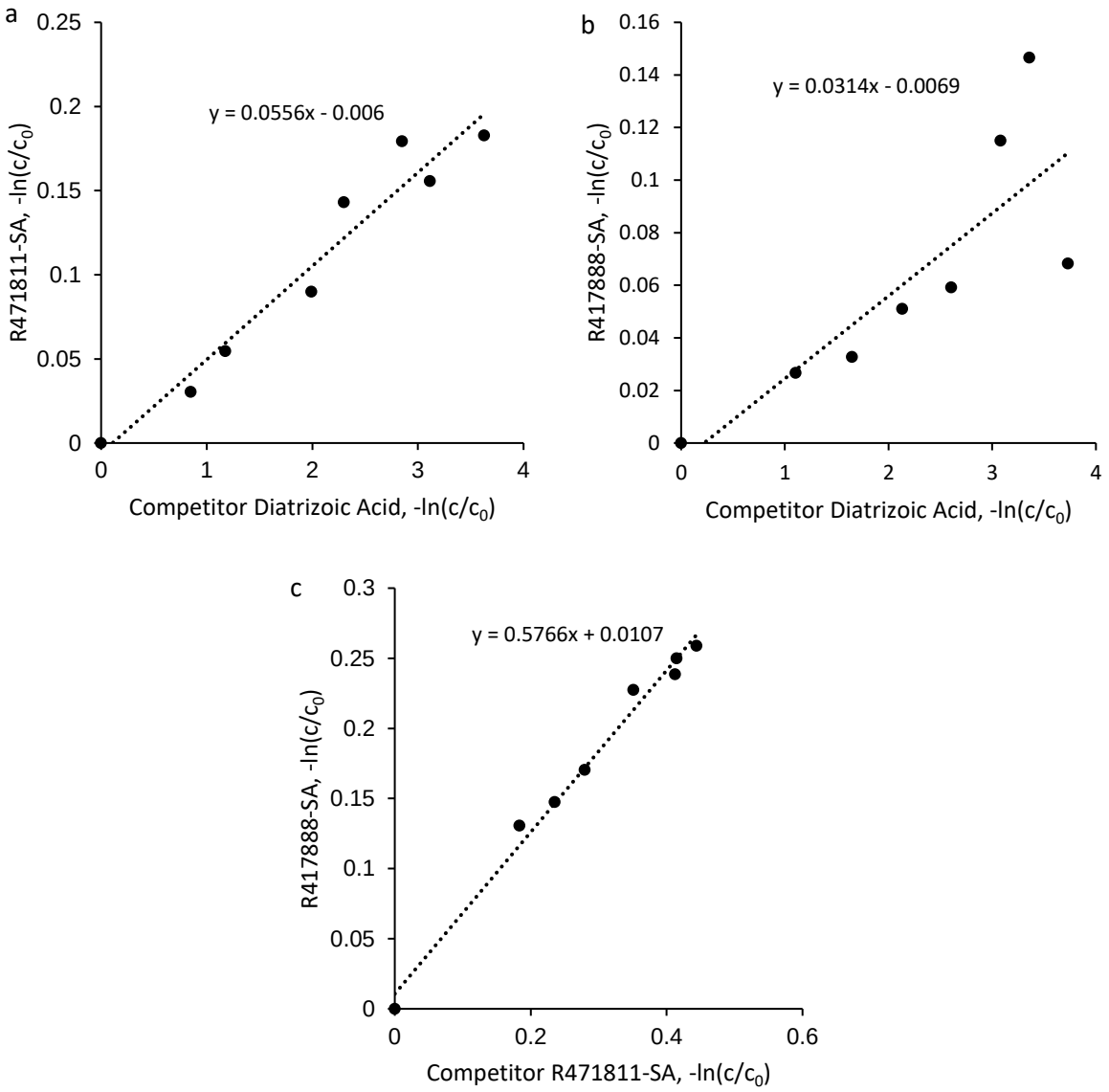

Figure SI-A5: Competition kinetics plot (a, b) for the sulfonic acid TPs and the competitor diatrizoic acid and (c) for the two sulfonic acid TPs during ozonation at pH ~10 (reaction by ·OH). Temperature: 23 ± 2 °C. Concentration of TPs and competitor: 1 µM.

SI-A9: Advanced Oxidation Experiments with Phenols

Degradation of the phenolic TPs by advanced oxidation was investigated using the UVA/H_2O_2 method. The phenolic TPs (0.1 µM) were exposed to UVA irradiation (350-410 nm, emission peak 367 nm, eight lamps) in a merry-go-round photoreactor (Rayonet, Southern New England Ultraviolet Company, Branford, USA) for 180 min together with the competitor benzoic acid (10 µM, $k_{OH} = 5.9 \times 10^9\ M^{-1}\ s^{-1}$, Buxton et al. (1988)) in presence of H_2O_2 (1 mM). In addition, the TPs were irradiated without H_2O_2 and benzoic acid to quantify direct photodegradation. Experiments were conducted in triplicate. Controls with H_2O_2 in the dark were stable, but the phenolic TPs were transformed during UVA irradiation in the absence of H_2O_2. The TP R611968-Ph was degraded faster by UVA/H_2O_2 than by UVA irradiation, whereas, the TP SYN507900-Ph was degraded approximately as fast by UVA irradiation as by UVA/H_2O_2 (Figure SI-A6). Therefore, the second order rate constant k_{OH} could not be determined for SYN507900-Ph.

In case of R611968-Ph, first the degradation by ˙OH was determined according to equation (SI-19):

$$\frac{[TP]_t}{[TP]_{0\ \underset{Radicals}{OH}}} = 1 - \left(\frac{[TP]_t}{[TP]_{0_{UVA}}} - \frac{[TP]_t}{[TP]_{0_{UVA/H2O2}}} \right) \quad \text{(SI-19)}$$

where [TP] describes the concentration of R611968-Ph at different time points. Competition kinetics plots were generated by plotting the logarithmically normalized decrease of TPs, $\ln(C/C_0)$, against the logarithm of the relative residual concentration of benzoic acid and k_{OH}^{TP} was determined from the slope of the linear regression model:

$$\ln\left(\frac{[TP]_t}{[TP]_{0\ \underset{Radicals}{OH}}} \right) = \frac{k_{OH}^{TP}}{k_{OH}^{benzoic\ acid}} \ln\left(\frac{[benzoic\ acid]_t}{[benzoic\ acid]_0} \right) \quad \text{(SI-20)}$$

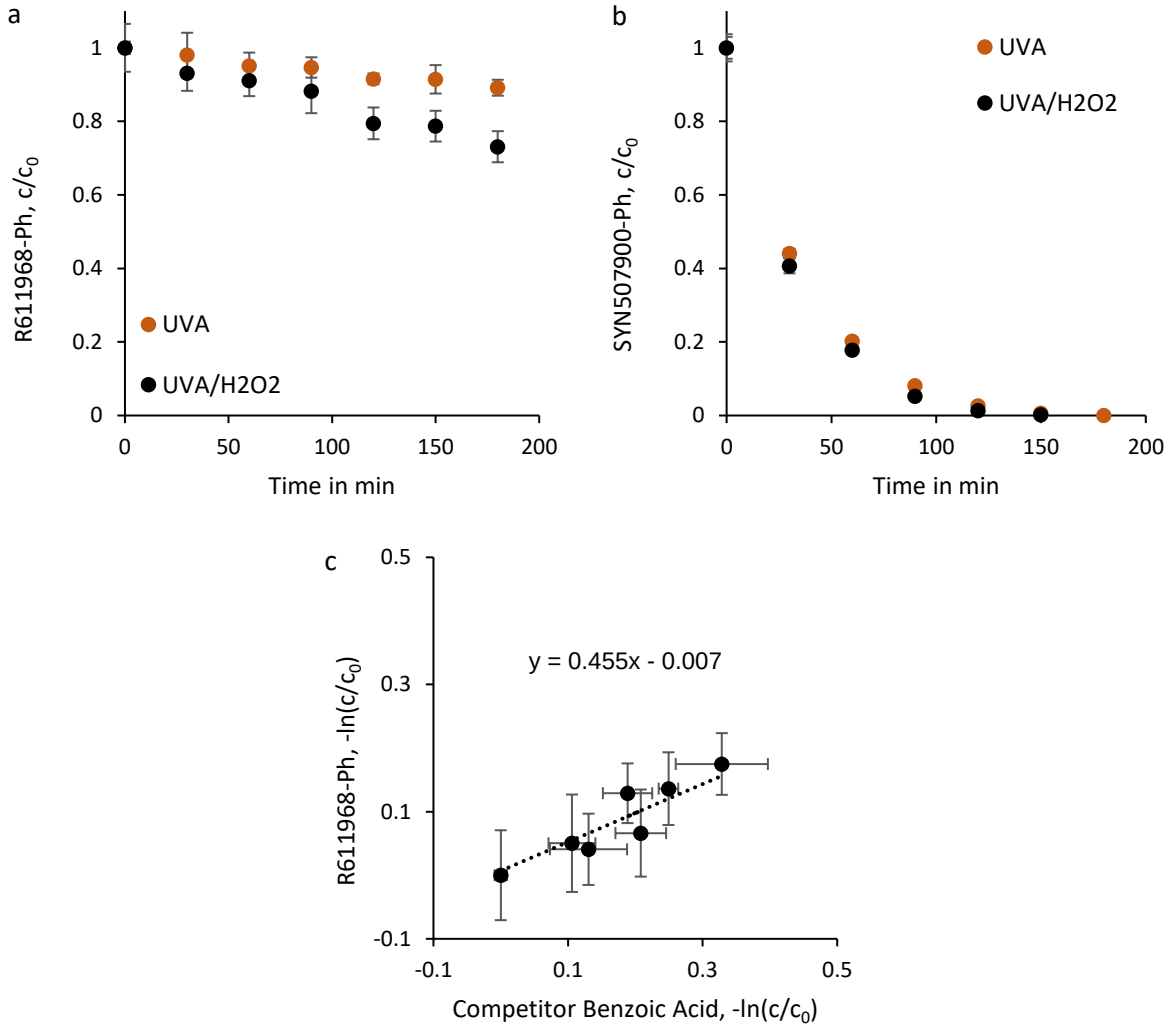

Figure SI-A6: Degradation of (a) R611968-Ph and (b) SYN507900-Ph by UVA and UVA/H_2O_2. (c) Competition kinetics plot for R611968-Ph and the competitor benzoic acid in the UVA/H_2O_2 process (˙OH). Degradation of R611968-Ph was corrected for abatement by UVA irradiation only. Error bars indicate the standard deviation of experimental triplicates. Temperature: 12 ± 2 °C. pH: 7.5 (5 mM phosphate buffer). Chlorothalonil TPs: 0.1 µM.

SI-A10: Adsorption on Activated Carbon

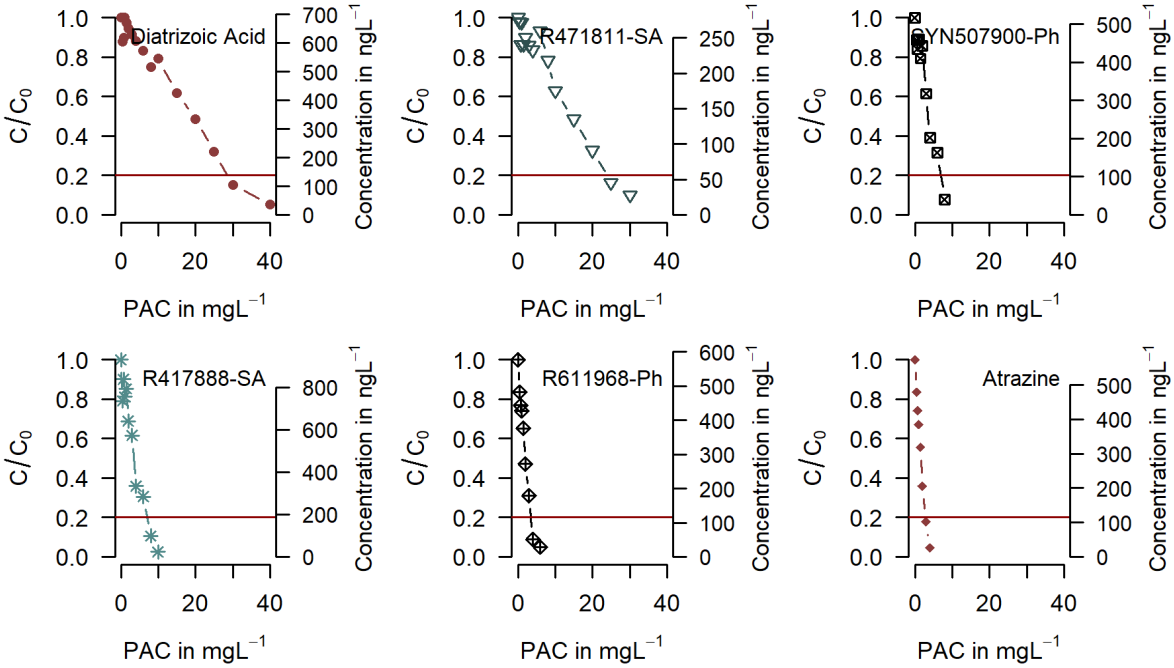

Figure SI-A7: Abatement of chlorothalonil TPs, diatrizoic acid, and atrazine as a function of powdered activated carbon (PAC) dosed into natural groundwater (multi-component system) after 42 h. Red line marks 80% removal. Powdered activated carbon: Eurocarb CC PHO 8x30 produced from coconut shell. Temperature: 22 °C. Dissolved organic carbon content: 1.1 mgL^{-1}. Electrical conductivity: 840 μScm^{-1}.

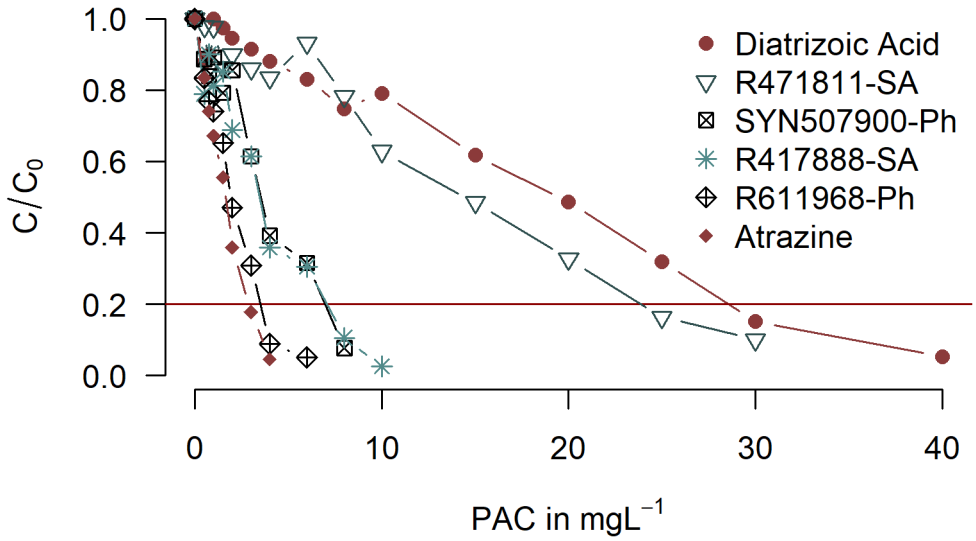

Figure SI-A 8: Abatement of chlorothalonil TPs, diatrizoic acid, and atrazine by different powdered activated carbon (PAC) dosed into natural groundwater (multi-component system) after 42 h. Red line marks 80% removal. Powdered activated carbon: Eurocarb CC PHO 8x30. Temperature: 22 °C. Dissolved organic carbon content: 1.1 mgL^{-1}. Electrical conductivity: 840 μScm^{-1}.

SI-A11: Confirmation of the R417888-SA isomer: SYN548581-SA

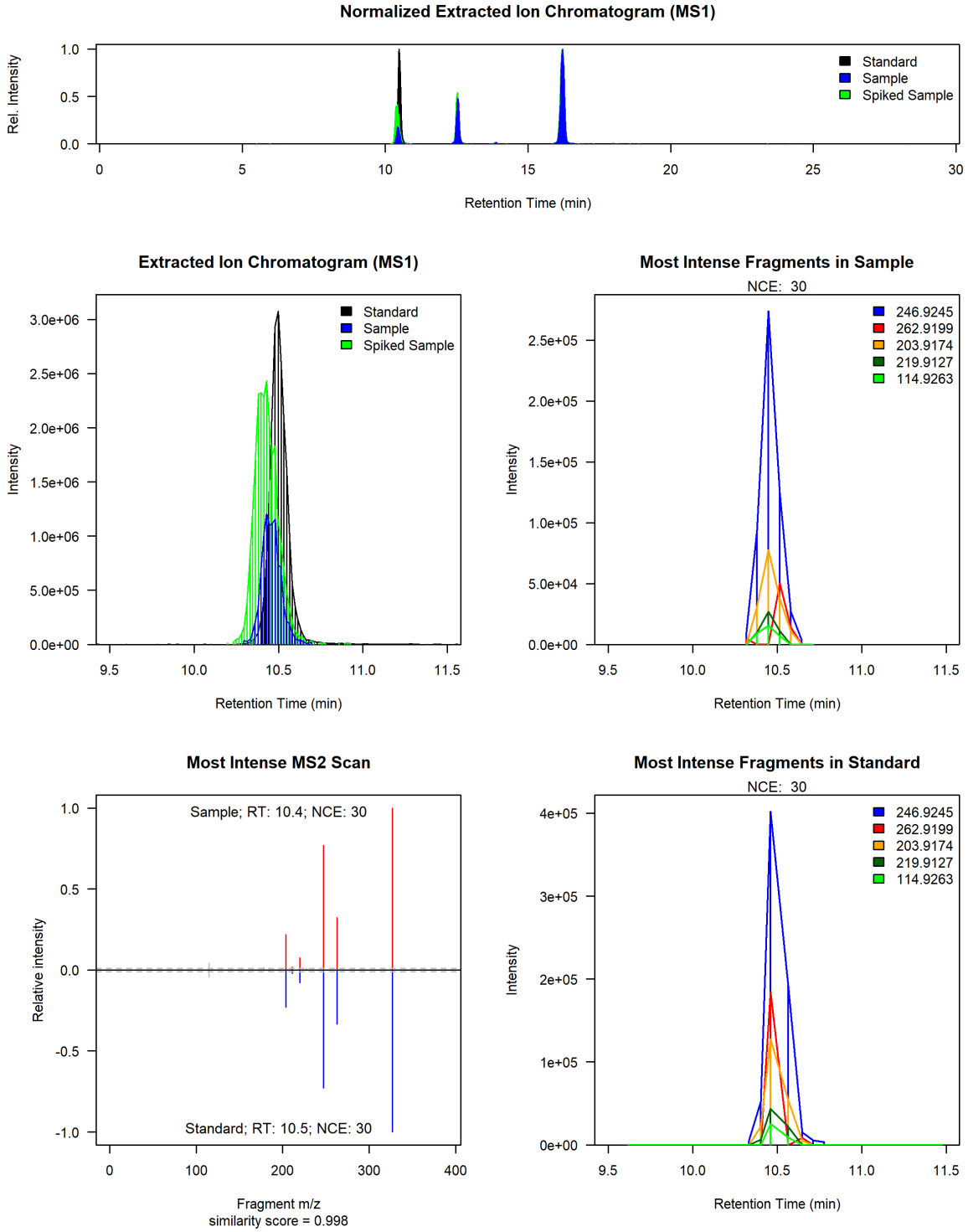

Figure SI-A9: SYN548581 (isomer of R417888-SA) was confirmed with reference material. The normalized extracted ion chromatogram (m/z 326.88063, 5 ppm window) shows three chromatographic peaks in the sample (blue). The sample was spiked with SYN548581 (green) so that the first peak (retention time 10.5 min) was identified as SYN548581. MS/MS fragments confirm the identification. R417888-SA elutes at 16 min. The compound eluting at 12.5 min is assumed to be another isomer of R417888-SA, which so far could not be confirmed.

References

Bader, H. and Hoigné, J., 1981. Determination of ozone in water by the indigo method. Water research 15(4), 449-456.

Bahnmüller, S., Loi, C.H., Linge, K.L., Gunten, U. and Canonica, S., 2015. Degradation rates of benzotriazoles and benzothiazoles under UV-C irradiation and the advanced oxidation process UV/H2O2. Water Res 74, 143-154.

Buxton, G.V., Greenstock, C.L., Helman, W.P. and Ross, A.B., 1988. Critical Review of rate constants for reactions of hydrated electrons, hydrogen atoms and hydroxyl radicals (·OH/·O− in Aqueous Solution. 17(2), 513-886.

Canonica, S., Meunier, L. and von Gunten, U., 2008. Phototransformation of selected pharmaceuticals during UV treatment of drinking water.

Hessler, D.P., Gorenflo, V. and Frimmel, F.H., 1993. Degradation of Aqueous Atrazine and Metazachlor Solutions by UV and UV/H202 - Influence of pH and Herbicide Concentration. Acta hydrochimica et hydrobiologica 21(4), 209-214.

Hoigné, J. and Bader, H., 1983. Rate constants of reactions of ozone with organic and inorganic compounds in water—II: Dissociating organic compounds. Water research 17(2), 185-194.

Hoigné, J. and Bader, H., 1994. Characterization Of Water Quality Criteria for Ozonation Processes. Part II: Lifetime of Added Ozone. Ozone: Science & Engineering 16(2), 121-134.

Lee, Y. and von Gunten, U., 2012. Quantitative structure-activity relationships (QSARs) for the transformation of organic micropollutants during oxidative water treatment. Water Res 46(19), 6177-6195.

Nick, K., Schöler, H.F., Mark, G., Söylemez, T., Akhlaq, M.S., Schuchmann, H.-P. and Von Sonntag, C., 1992. Degradation of some triazine herbicides by UV radiation such as used in the UV disinfection of drinking water. J. Water Supply Res. Technol. Aqua 41(2), 82-87.

R Core Team, 2016. R: A language and environment for statistical computing. R Foundation for Statistical Computing, Vienna, Austria. https://www.R-project.org/.

Real, F.J., Benitez, F.J., Acero, J.L., Sagasti, J.J.P. and Casas, F., 2009. Kinetics of the Chemical Oxidation of the Pharmaceuticals Primidone, Ketoprofen, and Diatrizoate in Ultrapure and Natural Waters. Industrial & Engineering Chemistry Research 48(7), 3380-3388.

Schollée, J.E., 2018. TFAnalyzeR, version 1.0.1, Analysis of TraceFinder Target Screening, Zenodo, DOI: 10.5281/zenodo.3234748.

von Gunten, U. and Hoigne, J., 1994. Bromate Formation during Ozonization of Bromide-Containing Waters: Interaction of Ozone and Hydroxyl Radical Reactions. Environmental science & technology 28(7), 1234-1242.

von Sonntag, C. and von Gunten, U., 2012. Chemistry of Ozone in Water and Wastewater Treatment: From Basic Principles to Applications, IWA Publisher, London.